

## Mechanical Properties and Microstructural Analysis of AISI 316 During Different Types of Welding Processes: A Review

Neelesh Kumar\*, Mayank Kumar, Nitin Sharma, Piyush Shah, Ranganath M. S., R.S. Mishra  
 (Delhi Technological University, Delhi, India )  
 \*Email: [neeeleshk1996@gmail.com](mailto:neeeleshk1996@gmail.com)

**Abstract :** *Quality and productivity play important role in today's manufacturing market. The main objective of industries reveals with producing better quality product at minimum cost and increase productivity. Welding is the most vital and common operation use for joining of two similar and dissimilar parts. In this paper an overview of current research in welding of stainless steel 316 has been presented. Fundamental concepts and definitions commonly used in welding are introduced, including a background on the properties of SS 316. An outline of applications in mechanical engineering is presented. The analysis tools that are currently available to aid in design and analyse are also described. The goal of this review is to introduce the possibilities for further research in this field, and encourage future SS 316 welded designs and applications.*

**Keywords:** *316 stainless steel, Friction Stir Welding, Taguchi, Resistance spot welding, friction welding, laser welding, TIG welding, Finite Element Analysis, XRD, WDX/EDX ,SEM.*

### INTRODUCTION

Austenite Stainless Steel: Austenitic stainless steels are probably the most commonly used material of all the stainless steels and accounts for more than 70% of production. These include the 200 and 300 series. Basic composition of austenitic stainless steel is 18% chromium and 8% nickel. They are non-magnetic and non-hardenable by heat treatment. However, they can be hardened significantly by cold working. Austenitic stainless steels are further defined by the carbon content as; "L" grades, straight grades and "H" grades. The L

grades contain  $\leq 0.03$  wt. % C, the straight grades contain 0.03–0.08 wt. % C and the H grades contain anywhere from 0.04–0.10 wt. % C.

In this paper, weldability of AISI 316 has been discussed. AISI 316 is more resistant to certain corrosive conditions than the standard non-molybdenum bearing austenitic stainless steel. Mechanical and chemical properties of AISI316 are presented in Table 1 and Table 2 respectively. These are suitable where protection is required from highly corrosive non-oxidising acids.

**Table 1a: Mechanical properties of AISI 316[t]**

Density (kg/m <sup>3</sup> )	Elastic Modulus (GPa)	Mean Expansion 0-100°C	Co-efficient of Expansion 0-315°C	Thermal Expansion 0-580°C	Thermal Conductivity (W/m.K) At 100°C	Thermal Conductivity (W/m.K) At 500°C	Specific Heat 0-100°C (J/kg.K)	Electrical Resistivity (n Ω.m)
8000	193	15.9	16.2	17.5	16.3	21.5	500	740

AISI 316 is used for plant and equipment in chemical manufacture. 316 has moderate deep drawing and cold forming properties and able to be welded in thickness up to 12mm without subsequent heat treatment for most applications. AISI 316 is extensively used in exterior applications subject to severe industrial or marine atmospheres; chemical; textile; photographic and paper making equipment; wine vats. AISI 316L is an extra low carbon modification for 316, with similar corrosion resistance. Intended for heavier sheet or plate fabrication where welding without subsequent heat treatment is required. These can be welded in heavy sections without the risk of inter-granular corrosion in

the as-welded condition and also in the stress relieved condition under most circumstances. 316L is used in Chemical plant and food processing equipment.[1].

#### *Welding Austenite Stainless Steel*

The austenitic stainless steels are considered to be the most weldable of the stainless steels. They are routinely joined by all fusion and resistance welding processes. But there are two problems that are associated with welds in the austenitic stainless steels:

- 1) Sensitization of the weld heat affected zone, and
- 2) Hot cracking of weld metal.

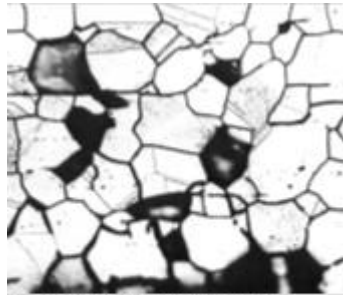


Figure 1: Intergranular corrosion [Sensitization][2]

Table 2. Chemical Composition

Element	TYPE 316	TYPE 316L
	%	%
Carbon	0.08 max.	0.03 max.
Manganese	2.00 max.	2.00 max.
Phosphorus	0.045 max.	0.045 max.
Sulphur	0.030 max.	0.03 max.
Silicon	0.75 max.	0.75 max.
Chromium	16.00 -18.00	16.00 - 18.00
Nickel	10.00 -14.00	10.00 -14.00
Molybdenum	2.00 - 3.00	2.00 - 3.00
Nitrogen	0.10 max.	0.10 max
Iron	Balance	Balance

### Sensitization

Sensitization is caused by chromium carbide formation and precipitation at grain boundaries in the heat affected zone when heated in the 800 to 1600°F (427 to 871°C) temperature range. Since most carbon is found near grain boundaries, chromium carbide formation removes some chromium from solution near the grain boundaries thereby reducing the corrosion resistance of these local areas. This problem can be remedied by using low carbon base material and filler material to reduce the amount of carbon available to combine with chromium. Carbide precipitation can be controlled by either using ELC (Extra Low Carbon) Grades (like 304L, 308L) or stabilized grades (like 321,347,348). Stabilized grades contain small elements like titanium, niobium which have a stronger affinity for carbon then does chromium leaving the chromium to provide corrosion [2].

Table 1b. Mechanical properties Of SS316[t]

Tensile strength (MPa) (min)	Yield Stress (MPa) (min)	Stress Elongation Proof (%50mm) (min)	Brinell Hardness (max)	Hardness in Rockwell B (HR B) (max)
515	205	40	217	217

### Hot (solidification) cracking

Hot cracking is caused by penetrating of grain boundaries by low melting materials such as sulphur and phosphorous and thus crack will appear as the weld cools and shrinkage stresses develop. Hot cracking can be prevented by adjusting the composition of the base material and filler material to obtain a microstructure with a small amount of ferrite in the austenite matrix. The ferrite provides ferrite austenite grain boundaries which are able to control the sulphur and phosphorous compounds so they do not permit hot cracking[2]. Solidification cracks can appear in several locations, and orientations, but most commonly are longitudinal centreline cracks (coincident with the intersection of grains growing from opposite sides of the weld), or 'flare' cracks, again longitudinal, but at an angle to the through-thickness direction ( Fig.2). Where there is a central segregate band in the plate, cracking may extend from this position at the fusion boundary ( Fig.3). The cracks in all locations can be buried (Fig.4) or surface-breaking[3]

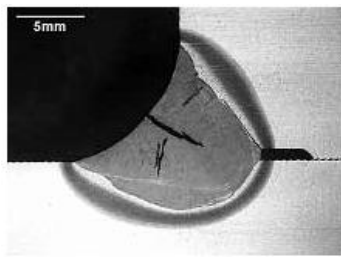


Figure2:Typical location of centreline

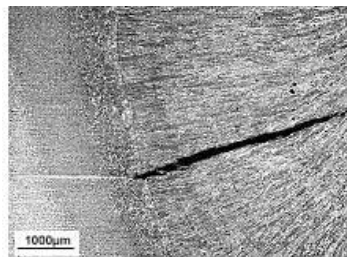


Figure 3:Cracking initiating from segregation flare solidification cracks[3]

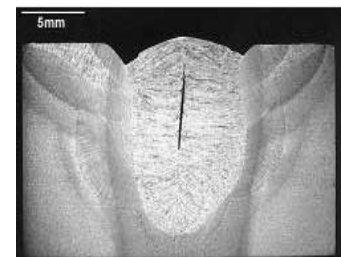


Figure 4: Buried centreline cracking[3]and band in plate[3]

### Different Welding Methods:

There are different methods of welding that are used to Austenite steels such as friction welding, laser beam welding, resistance spot welding, TIG welding, GMAW. Friction-stir welding (FSW) is a solid-state joining process (the metal is not melted) that uses a third body tool to join two facing surfaces. Heat is generated by friction between the tool and material which leads to a very soft region near

the FSW tool. It then mechanically intermixes the two pieces of metal at the place of the joint, then the softened metal (due to the elevated temperature) can be joined using mechanical pressure (which is applied by the tool), much like joining clay, or dough. It was invented and experimentally proven at The Welding Institute UK in December 1991. [4].

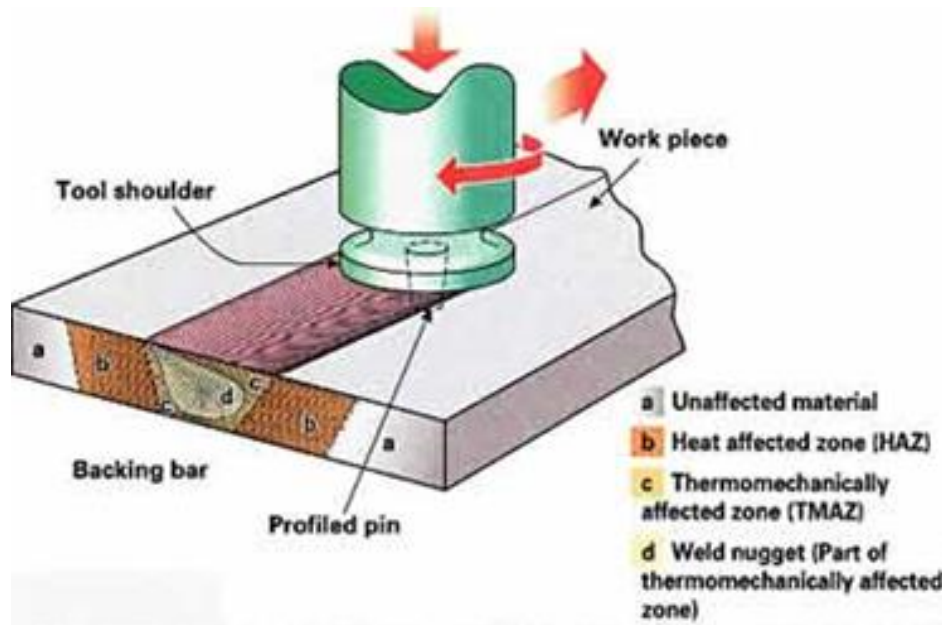


Figure 5: Friction Stir Welding (3)

Resistance spot welding is performed by using heat which is produced from resistance to current. This heat is used to join two metal surfaces. The advantages of resistance spot welding are that it is a cheap process, it provide dimensional accuracy and high speed process. There are also limitation of the process such as the tensile strength and fatigue strength is low, increase he weight and hard to repair [5]. Laser beam welding (LBW) is a welding process which produces coalescence of materials with the heat obtained from the application of a concentrate coherent light beam impinging upon the surfaces to be joined.[6]

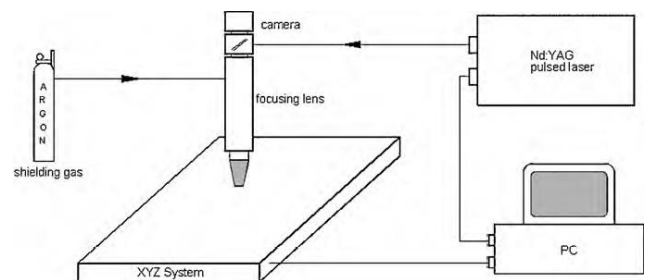


Figure 7: Schematic of typical pulsed Nd:YAG laser welding system[17]

Gas Tungsten Arc welding is an arc welding process which produces coalescence of metals by heating them with an arc between a tungsten (non-consumable) electrode and the work piece. Shielding is obtained from a gas or gas mixture[7]. Gas Metal Arc Welding is an arc welding process which produces coalescence of metals by heating them with an arc between a continuous filler metal (consumable) electrode and the work piece. Shielding is obtained entirely from an externally supplied gas or gas mixture. The electrode wire for GMAW is continuously fed into the arc and deposited as weld metal. This process has many variations depending on the type of shielding gas, the type of metal transfer, and the type of metal welded [5].

*Commonly used Analysis Tools:*

*Finite Element Method (FEM)* is a numerical technique for finding approximate solutions to boundary value problems for partial differential equations. It is also referred to as finite element analysis (FEA). It subdivides a large problem into smaller, simpler parts that are called finite elements. The simple equations that model these finite elements are then assembled into a larger system of equations that models the entire problem. FEM then uses variational methods from the calculus of variations to

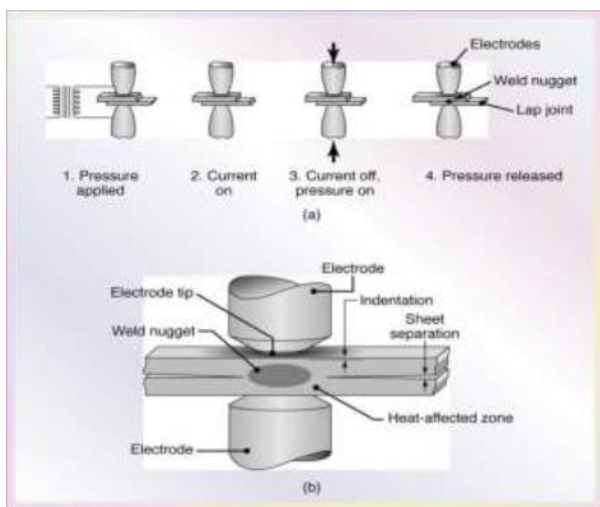


Figure 6: Resistance Spot Welding [16]

approximate a solution by minimizing an associated error function.[4]

*X-ray powder diffraction (XRD)* is a rapid analytical technique primarily used for phase identification of a crystalline material and can provide information on unit cell dimensions. X-ray diffraction is based on constructive interference of monochromatic X-rays and a crystalline sample. These X-rays are generated by a cathode ray tube, filtered to produce monochromatic radiation, collimated to concentrate, and directed toward the sample. The interaction of the incident rays with the sample produces constructive interference (and a diffracted ray) when conditions satisfy Bragg's Law ( $n\lambda=2d \sin \theta$ ). This law relates the wavelength of electromagnetic radiation to the diffraction angle and the lattice spacing in a crystalline sample. These diffracted X-rays are then detected, processed and counted. By scanning the sample through a range of  $2\theta$  angles, all possible diffraction directions of the lattice should be attained due to the random orientation of the powdered material. Conversion of the diffraction peaks to d-spacings allows identification of the mineral because each mineral has a set of unique d-spacings.[8]

*The scanning electron microscope (SEM)* uses a focused beam of high-energy electrons to generate a variety of signals at the surface of solid specimens. The signals that derive from electron-sample interactions reveal information about the sample including external morphology (texture), chemical composition, and crystalline structure and orientation of materials making up the sample.[4]

*Energy-Dispersive Spectroscopy (EDS):* Interaction of an electron beam with a sample target produces a variety of emissions, including x-rays. An EDS Detector is used to separate the characteristic x-rays of different elements into an energy spectrum, and EDS system software is used to analyse the energy spectrum in order to determine the abundance of specific elements. EDS can be used to find the chemical composition of materials down to a spot size of a few microns, and provide fundamental compositional information for a wide variety of materials.[8]

*Analysis of variance (ANOVA)* is a collection of statistical models used to analyse the differences among group means and their associated procedures. In its simplest form, ANOVA provides a statistical test of whether or not the means of several groups are equal, and therefore generalizes the t-test to more than two groups. ANOVAs are useful for comparing (testing) three or more means (groups or variables) for statistical significance. It is conceptually similar to multiple two-sample t-tests, but is more conservative (results in less type I error) and is therefore suited to a wide range of practical problems.[8]

*TAGUCHI Method:* Dr. Genichi Taguchi of Nippon Telephones and Telegraph Company, Japan has developed

a method based on "Orthogonal Array" experiments which gives much reduced variance for the experiment with optimum settings of control parameters. Thus the combination of design of experiments with optimization of control parameters to obtain best results is achieved in the Taguchi Method. "Orthogonal Arrays" (OA) provide a set of well balanced (minimum) experiments and Dr. Taguchi's Signal-to-Noise ratios (S/N), which are log functions of desired output, serve as objective functions for optimization, help in data analysis and prediction of optimum results. These are used to improve the quality of manufactured goods, engineering, biotechnology, marketing and advertising.[9][4]

*Laser-induced breakdown spectroscopy (LIBS)* is a type of atomic emission spectroscopy which uses a highly energetic laser pulse as the excitation source. The laser is focused to form plasma, which atomizes and excites samples. In principle, LIBS can analyse any matter regardless of its physical state, be it solid, liquid or gas because all elements emit light of characteristic frequencies when excited to sufficiently high temperatures. So LIBS can (in principle) detect all elements, limited only by the power of the laser as well as the sensitivity and wavelength range of the spectrograph & detector. If the constituents of a material to be analysed are known, LIBS may be used to evaluate the relative abundance of each constituent element, or to monitor the presence of impurities.[4]

Energy-dispersive X-ray spectroscopy (EDS, EDX, or XEDS), sometimes called energy dispersive X-ray analysis (EDXA) or energy dispersive X-ray microanalysis (EDXMA), is an analytical technique used for the elemental analysis or chemical characterization of a sample. It relies on an interaction of some source of X-ray excitation and a sample. Its characterization capabilities are due in large part to the fundamental principle that each element has a unique atomic structure allowing a unique set of peaks on its electromagnetic emission spectrum.[4]

Wavelength-dispersive X-ray spectroscopy (WDXRF or WDS) is a method used to count the number of X-rays of a specific wavelength diffracted by a crystal. The wavelength of the impinging X-ray and the crystal's lattice spacings are related by Bragg's law and produce constructive interference if they fit the criteria of Bragg's law. Unlike the related technique of energy-dispersive X-ray spectroscopy (EDS), WDS reads or counts only the X-rays of a single wavelength at a time, not producing a broad spectrum of wavelengths or energies simultaneously. WDS is mainly used in chemical analysis, in an X-ray fluorescence spectrometer, in an electron microprobe, and may be used in a scanning electron microscope.[4]

**Literature Review of Different types of Welding on AISI 316:**

Ref No.	Materials Welded	Welding	Machines & Tool Used	Parameters (Optimum)	Analysis tools	Results And Significant findings
10.	AISI 316L Square bars	Linear Resistance Welding	Electromechanical LFW machine	<b>Frequency</b> ( 45,40, 25 HZ ) <b>Amplitude</b> ( $\pm 3, 2.5, 1$ mm) <b>Friction pressure</b> ( 240, 160, 60MPa) <b>Burn-off distance</b> ( 3 , 1 mm) <b>Forge Pressure</b> (same as friction pressure for 5s)	Optical microscopy , texture analysis using synchrotron X-ray diffraction(XRD) , tensile strength test	<b>UTS:</b> 512-610 MPa <b>Failure Location:</b> Parent Material region The <b>burn-off rate</b> has a very large effect on the final $\delta$ - ferrite fraction, with high burn-off rates producing low levels of $\delta$ -ferrite.
11.	AISI 316L plates	Resistance Spot Welding	AC spot welding Machine, water cooled conical Cu-Cr electrodes	<b>Weld Time:</b> 10, 15, 20 cycles (1 cycle = 0.02 s) <b>Weld current</b> (7 kA) <b>Applied electrode pressure</b> ( $6 \times 10^5$ Pa) <b>Holding time of electrode</b> (30 cycles) <b>Cooling atm.</b> :air, nitrogen ,10% Borax	Optical microscopy , tensile shear strength test, micro-hardness test	<b>Tensile Shear Strength:</b> Nitrogen>Air>10% Borax <b>Max. Joint Strength:</b> 20 cycles Failure: Excessive grain growth of HAZ The <b>tensile shear load bearing capacity</b> of welded samples increased with increasing heat input related with weld time due to the enlargement of nugget size.
12	SS316 Repair keyhole	filling friction stir welding (FFSW)	Filling Tool:SS316	<b>Rotation speed</b> : 1500rpm <b>Applied Force:</b> 30KN <b>Holding Time:</b> 5,10s	optical microscopy ,transmission electron microscopy, transverse tensile strength test	<b>Fracture:</b> interface of the refilled joint <b>No <math>\sigma</math> phase</b> but few Cr carbides was developed at the interface of refilled keyhole Typical relative <b>Tensile strength</b> and <b>elongation</b> are significantly lower than those of the as-received plate for defects formed at the refilled joint interface.
13	SS316L and Cu plates	FSW	WC-14Co Tool	<b>Spindle Speed:</b> 1000, 1500 rpm <b>Welding Speed:</b> 100 ,200, 300 mm/min <b>Tool Offset</b> :0,0.6,1.6mm	Microstructural characterization, transverse tensile, and Vickers microhardness	<b>UTS</b> (170-267 MPa) lower than Cu (306MPa) <b>Failure:</b> bi-metallic interface Increasing the offset compromises the robustness resulting in void formation, lower tensile strength and elongation
14	AISI 316L plates	FSW	<b>Tool T1</b> (99%)W-(1%) La2O3  <b>Tool T2</b> (90.12%) W-(5.97%) Ni-(3.56%) Fe-(0.22%) Mo-(0.15%) Co	<b>Spindle Speed:</b> 600 rpm <b>Welding Speed:</b> 45mm/min <b>Axial Force:</b> 11KN <b>Tilt angle:</b> 1.5°	Optical microscopy, Scanning Electron Micrograph (SEM) and Energy Dispersive Spectrometer (EDS) analysis, Microhardness test , tensile strength test , tool degradation study by mass loss and photographic techniques	<b>Tool wear</b> T1: 12g& T2: 189g <b>UTS</b> T1:609 $\pm$ 8 MPa (joint efficiency of 96 $\pm$ 1.3%) <b>UTS</b> T2: 542 $\pm$ 6 MPa ( joint efficiency of 86 $\pm$ 1%) <b>Yield Strength</b> increased for both tools, No sign of <b>sigma phase</b> formation was observed, <b>Joint Efficiency</b> was affected by the distribution of tungsten tool wear debris in the weld stir zone.
15	6063 Al Alloy & SS316L	Spot Welding		<b>Current:</b> 4 kA, 5 kA, 6 kA <b>Welding Cycle:</b> 10 cycles <b>Force</b> :1500 N	Tensile Shear load test, Vicker's hardness test	Tensile shear strength of the joints increases as the welding current increases. The relationship between the nugget diameter and the welding current reveals that tensile shear load solely relies on the size of the welding nugget.
16	AISI 316L sheets	Resistance Spot Welding	3 phase DC pedestal type	<b>Electrode Tip Dia:</b> 6,7,8mm <b>Welding Current:</b> 7,8,9kA <b>Heating time:</b> 7,8,9 cycles	Tensile Shear Test	Maximum load carried by the joint was obtained at 7 mm electrode spot diameter

			resistance spot welding machine	<b>Electrode force:</b> 3.2 kN <b>Squeeze time:</b> 10 cycles <b>Hold time:</b> 10 cycles		and 9 kA welding current in 9 cycles heating time. Types of breaking failure: (1) knotting, (2) separation and (3)tearing, Nugget Dia increases with welding current								
17	AISI 316L Thin foil	Laser Beam Welding	Pulsed Nd:YAG laser system	<b>Beam spot size :</b> 0.2mm <b>Beam angle :</b> 90° <b>Welding speed :</b> 525mm/min <b>Repetition rate (Rr):</b> 39 Hz <b>Pulse energy (Ep):</b> 1.0 to 2.25 J at increments of 0.25 J with a 4ms <b>pulse duration (tp).</b>	Optical microscopy, Vickers micro-hardness and tensile shear strength tests.	<b>UTS</b> of the welded joints initially increased and then decreased as the pulse energy increased.								
18	AISI 316L & Al 5083-H321	FSW	H13 steel tool	<b>Rotational speed:</b> 280rpm <b>Traverse speed:</b> 160 mm/min <b>Pin offset</b> :-0.4,0, +0.4,0.8, 1 mm <b>Tilt Angle:</b> 2.5°	Taguchi Method, ANOVA , Tensile strength test , optical microscopy	<ul style="list-style-type: none"> <li>• Increase in Traverse speed lead to formation of tunnel and void defect</li> <li>• Increasing the pin offset value from negative to values cause to increase of tensile strength up to a maximum amount and then decrease</li> <li>• The highest and lowest hardness values belong to the steel TMAZ and the Al HAZ, respectively.</li> <li>• The FeAl3 intermetallic compounds form in the dispersed steel fragments and Al interface during FSW.</li> </ul>								
19	AISI 316	FSW	ETA Welding M/c ,Tool Q70	<b>RPM :</b> 1100 <b>Welding Speed :</b> 8mm/min <b>Plunge depth :</b> 3.72mm <b>Tilt angle =</b> 2°	Optical Microscopy, Vicker's Hardness Tests and tensile tests.	Defect free weld; <b>UTS value higher</b> than bas material with increased hardness in nugget zone.								
20	AA1100, SS316	RFW		<b>RPM =</b> 2000 <b>Frictional time =</b> 5 sec <b>Frictional pressure =</b> 80 MPa <b>Forging pressure =</b> 160 MPa	ANSYS, ANOVA, Finite Element Modelling (FEM), Taguchi	Good welding results. <b>Forging pressure should be higher than the frictional pressure</b> <b>Good penetration and sliding</b> of materials at the welding interface								
21	SS316, EN8	FSW	FWT-12	<b>RPM =</b> 1580 <b>Cooling =</b> Oil quenching <b>Forging Pressure =</b> 28 Bar	Taguchi, ANOVA, Minitab	Forging Pressure has the greatest influence on the S/N ratio, followed by rotational speed then cooling method.								
22	HSS M <sub>33</sub> , SS316	Continuous Drive friction welding	Lathe M/C	<table border="1"> <thead> <tr> <th>RP M</th> <th>Breaking Load (KN)</th> </tr> </thead> <tbody> <tr> <td>1700</td> <td>9.96 (HSS rpm &amp; SS constant.) 3.82(HSS constant &amp; SS rpm)</td> </tr> <tr> <td>2700</td> <td>9.10 (HSS rpm &amp; SS constant.) 2.92(HSS constant &amp; SS rpm)</td> </tr> <tr> <td>3700</td> <td>3.30 (HSS rpm &amp; SS constant.) 3.54 (HSS constant &amp; SS rpm)</td> </tr> </tbody> </table>	RP M	Breaking Load (KN)	1700	9.96 (HSS rpm & SS constant.) 3.82(HSS constant & SS rpm)	2700	9.10 (HSS rpm & SS constant.) 2.92(HSS constant & SS rpm)	3700	3.30 (HSS rpm & SS constant.) 3.54 (HSS constant & SS rpm)	Optical Microscopy	Good Strength of the joints obtained ; As RPM increases (HSS rpm & SS constant) of job then breaking point load decreases but when rpm (HSS constant & SS rpm) of job increases then breaking point load increases at high rpm.
RP M	Breaking Load (KN)													
1700	9.96 (HSS rpm & SS constant.) 3.82(HSS constant & SS rpm)													
2700	9.10 (HSS rpm & SS constant.) 2.92(HSS constant & SS rpm)													
3700	3.30 (HSS rpm & SS constant.) 3.54 (HSS constant & SS rpm)													
23	SS 316	FSW	ETA , Tool Q70	<b>RPM =</b> 1100 <b>Welding speed =</b> 8mm/min	Optical Microscopy, Tensile Test Plot	<b>104% of Base Material Mechanical Strength and</b>								

				<b>Plunge depth : 3.72mm</b>		<b>37% elongation</b> achieved.
24	Aluminium alloy 6061, SS316	FSW	SEM, UTM. Tool: SS 304, SS 316, MS	<b>RPM</b> (1000, 1100 and 1645) for <b>Tool materials</b> ( MS, SS304, SS316) <b>Weld Speed</b> (90,100,110) <b>Down Force</b> (10kN constant)	SEM, BHN vs Distance from weld centre Plot	SS 316 best tool for welding the alloy – better impact value, tensile strength.
25	SS 316, AI5754	LBW	Nd: YAG laser model IQL-10	<b>Laser welding of SS316:</b> <b>Pulse energy</b> (3 -18 Joules) <b>Pulse duration</b> (2 - 12ms) <b>Process speed</b> (5 mm/s constant) <b>Pulse repetition rate</b> (20 HZ constant) <b>Laser welding of Al 5754:</b> <b>Pulse energy</b> (4.5 - 10.5 Joules) <b>Pulse duration</b> (3 - 7ms) <b>Process speed</b> (9 mm/s constant) <b>Pulse repetition rate</b> (10 HZ constant)	Laser Induced Breakdown Spectroscopy (LIBS), Wavelength Dispersive X-Ray/Energy Dispersive X-Ray(WDX/EDX), Particle Induced X-Ray Emission(PIXE), Quick Calculus software (online)	Alloying elements are controlled in weld metal by changing the laser parameters ; Mn, Cr concentrations reduce within the weld metal however, those of Fe, Ni increase simultaneously ; Mg loss linearly increases with increasing the pulse duration of the laser welding; Variation of Mg trace is negligible while varying the laser power density.
26	6061 Al alloy, SS 316, Zn foil	FSW	Tool WC-13% Co	<b>RPM</b> (1200 rpm) <b>Traverse speed</b> (40 mm/min), <b>Plunge depth</b> (0.1 mm) <b>Welding Tool Title Angle</b> (2°) <b>Zn foil thickness</b> – 0.1 & 0.3 mm	SEM, XRD, EDS Quantitative Analysis	Sound lap joints achieved. No IMC layer is generated. Macro Interlocks give good strength.
27	SS 316LN	TIG	Automated TIG welding M/C,	<b>Argon shielding gas,</b> <b>Welding Speed</b> (100mm/min) <b>Arc Gap</b> (3mm) <b>Distortion</b> (3.5,4.0,4.5,5.0,5.5 mm), <b>Flow Rate</b> – 10 lt./hr	Finite element Analysis, XRD AND Ultrasonic Testing (UT)	At Quasi Steady state condition Temp.-1686 <sup>0</sup> , Heating rate-229.5 <sup>0</sup> C/s <sup>2</sup> , Cooling Rate--85.5 <sup>0</sup> C/s <sup>2</sup> Buckling deformation occurred – distorted plates due to release of clamps; FEM is a good predictive tool.
28	SS 316N, Duplex Stainless Steel (DSS)	TIG	Universal Testing Machine(UTM)	<b>Tensile Strength</b> (485,621,735MPa), <b>BHN</b> (210,260,293), <b>Yield Strength</b> (170,450,610MPa)	Microstructural Analysis, Impact Test, Tensile test, Hardness Analysis, Bending Test	Hardness of DSS is more than SS 316N, Welding results increase in T.S. & Y.S. but decrease in % Elongation
29	AISI 316LN	TIG-MAG	TIG Welding Machine	<b>Filler wire material</b> (ER316), <b>Sample Thickness</b> (5,10,20,30 mm), <b>Tensile Strength</b> (630,647,659,672 MPa), <b>No. Of Passes</b> (3,5,7), Root Gap(2mm)	Radiographic test, Stander Bending Test	Welded material is subjected to no defects like pores, voids, cracks & penetration, successfully subjected to bend test requirement.
30	AISI 316LN	TIG	Automated TIG welding Machine	<b>Longitudinal Distance from centreline/mm</b> (-100,-50,50,100)	FEM,IR Thermography UT, XRD, Residual stress Analysis	At Quasi Steady state condition Temp.-1686 <sup>0</sup> , Heating rate-229.5 <sup>0</sup> C/s <sup>2</sup> , Cooling Rate--85.5 <sup>0</sup> C/s <sup>2</sup> ,
31	AISI 316LN	Laser Beam Welding, TIG,A-TIG,MP-	TIG Welding Machine	<b>Filler Metal-AWS E/ER 209,</b> <b>Applied Stress</b> (125,150,175,200,225 MPa), <b>Rupture Time</b> (10,100,1000 h), <b>Distance from centre of the weld</b> (-4,-2,0,2,4 mm),	Curve b/w (a) reduction in area (%) and (b) elongation (%) with rupture time, Laser Welding Analysis Method	Reduction in bevel preparation requirements, Reduced consumption of welding filler wire, Reduced distortion, Reduced Magnitude of residual stress in A-TIG is less than MP-

		TIG				TIG
32	SS 316L	TIG	TIG Welding Machine	<b>Welding current</b> (150,180,210 A), <b>Welding Speed</b> (3.3,4.2,5mm/s <sup>2</sup> ), <b>Arc Length</b> (2, 3, 4 mm), <b>Optimal Parameter for max. penetration</b> (welding current-210 A, Arc length-2mm,electrode angle-75 <sup>0</sup> )	Taguchi Method, ANOVA	Activating fluxes improve the joint mechanical properties by decreasing the grain Size of heat affected zone, max. Arc voltage for SiO <sub>2</sub> flux
33	SS 316L	TIG Welding		<b>gas flow</b> (9 lit/s), <b>voltage</b> (9,11,13 V) , <b>Travel speed</b> (70mm/min), <b>current</b> (55 A), <b>Heat input</b> (518J/mm)	SEM, Post Weld Heat Treatment (PHWT), XRD Techniques	PHWT decreased the corrosion rate of the welded couple,
34	SS 316L	A-TIG ,M-TIG ,K-TIG ,U-TIG	Charge coupled device (CCD) camera, Ferritoscope, LECO TC-436 Apparatus	<b>Electrode type</b> -DCEN, W-2% ThO <sub>2</sub> , <b>Diameter of electrode</b> -3.2 mm, <b>Vertex angle of electrode</b> -60 <sup>0</sup> <b>Welding current</b> -150 A, <b>Welding speed</b> -150mm/min, <b>Arc length</b> - 3 mm, <b>Shielding gas</b> - Pure argon <b>Gas flow rate</b> - 12 L/min	Optical macrographs, Weld Morphology, SEM	The SiO <sub>2</sub> flux showed a greater ability to increase the weld penetration and D/W ratio than other fluxes , A-TIG can increase U.T.M., In the range of 70-150 ppm D/W Ratio Suddenly increased.
35	SS 316	TIG, Arc Welding	Rockwell Hardness Testing Machine, Black Diamond Cone Indenter, Impact tester	<b>Initial Energy</b> (E <sub>i</sub> )=300 KJ, <b>Minor Load</b> =150 kgf, <b>Speed</b> (800,900,950,1050 rpm),	Charpy Testing, Microstructure analysis, Micrograph	Increased microstructure improve ; Complete fusion structure and hardness Increased. Average Rockwell Hardness No.(52,59,62.4,63.2), Yield Strength (361.70,380,386.80,434.30 MPa), % Elongation (1.5,2,3,7 mm)

### CONCLUSIONS

Study of the mechanical properties of the weld is very important because the main purpose of the welding is to strongly join the two metals together as the application of the welded structure may be at sensitive place. It is important to check the tensile strength of the weld and the factors affecting the strength of the weld. The major problem which occurs in AISI316 welds is the formation of inter-metallic compounds at the interface which affect the properties and efficiency of the weld. Lap joints can be using filler metals (like Zn) without formation of IMC as they results in better strength, though the tool pin depth would also play a vital role.

In laser beam welding the better performance was due to the high quality joint marked by full penetration, no underfill and free from micro cracks and porosity. Loss of alloying elements strongly takes place at higher peak powers and longer pulse durations. The austenitic steel when subjected to laser welding, there will be problems like gas evolution unless the welding parameters are optimized. LIBS was found to be a good analysis tool for such processes. In resistance spot welding it was found

that the tensile shear load bearing capacity of welded samples increased with increasing heat input related with weld time due to the enlargement of nugget size. In TIG welding between dissimilar metals the welding is found to be in acceptable level. Activating fluxes improve the joint mechanical properties by decreasing the grain size of HAZ. TIG-MAG Welded samples exhibited good weld joint strength without any cracks, openings and porosity. A-TIG welding can increase ultimate tensile strength of weldments because of increasing the retained delta-ferrite content of stainless steel welds. In the above welding experiments, FSW is found to be most defect free welding. No intermetallic  $\sigma$ -phase was found in the weld in FSW. The precipitation of the  $\sigma$ -phase is the main reason for the degradation of stainless steels. Tensile testing results have confirmed that the mechanical properties of FSW of SS316 compare well with parent metal properties. Grains in nugget zone are completely distorted with no twin boundaries as in base material, because of the stirring action of the tool which can be attributed to dynamic crystallization. Considering economical aspects, manual the machine can also be used for the friction



welding operation. FSW between the dissimilar materials can be successfully carried out and the process can be optimized so that cheaper materials can be used in manufacturing and automotive industries to save huge amounts. Taguchi method for optimizing parameters, Infrared thermography, Finite Element Modelling and LIBS were found to be very effective tools for analysis. Concluding, further research work can be done on optimizing process parameters of FSW of SS316 and making a suitable mathematical model for the same.

## REFERENCES

1. Users Guide Stainless Steel , steel and tube industries ltd
2. Stainless Steel guide of Lincoln Electric
3. <https://www.twi-global.com/>
4. [www.wikipedia.org](http://www.wikipedia.org)
5. Welding of Dissimilar Metals, Article, Total Materia
6. <http://www.weldguru.com/Laser-Welding.html>].
7. Stainless Steel - Grade 316 (UNS S31600) , AZO materials
8. ....[http://serc.carleton.edu/research\\_education/geochemsheets/browse.html](http://serc.carleton.edu/research_education/geochemsheets/browse.html)
9. ....[https://www.ee.iitb.ac.in/~apte/CV\\_PRA\\_TAGUCHI\\_INTRO.htm](https://www.ee.iitb.ac.in/~apte/CV_PRA_TAGUCHI_INTRO.htm)
10. Imran Bhamjia, Michael Preussa, Philip L. Threadgill, Richard J. Moata, Adrian C. Addison, Matthew J. Peeld "Linear friction welding of AISI 316L stainless steel", *Materials Science and Engineering A* 528 (2010) 680-690
11. Bayram Kocabekir, Ramazan Kaçar, Süleyman Gündüz, Fatih Hayat "An effect of heat input, weld atmosphere and weld cooling conditions on the resistance spot weldability of 316L austenitic stainless steel" *Journal of materials processing technology* 195 (2008) 327-335
12. L. Zhou, & W. L. Zhou & Y. X. Huang & J. C. Feng "Interface behaviour and mechanical properties of 316L stainless steel filling friction stir welded joints" *Int J Adv Manuf Technol* (2015) 81:577-583
13. Antonio J Ramirez, Davi M Benati, Hipolito Fals "Effect of tool offset on dissimilar Cu-AISI 316 stainless steel friction stir welding"  
<https://www.researchgate.net/publication/289095201>
14. S. Shashi Kumar , N. Murugan, K.K. Ramachandran "Influence of tool material on mechanical and microstructural properties of friction stir welded 316L austenitic stainless steel butt joints", *Int. Journal of Refractory Metals and Hard Materials* 58 (2016) 196-205
15. Mazlee Mohd Noor, Alvin Tan Yin Zhen , Shamsul Baharin Jamaludin, Nur Farhana Hayazi , Shaiful Rizam Shamsudin - " Joining of Dissimilar 6063 Aluminium Alloy-316L Stainless Steel by Spot Welding: Tensile Shear Strength and Heat Treatment" *Advanced Materials Research* Vol. 795 (2013) pp 492-495
16. K. Gopalakrishnan, S. Gokulakrishnan - "Mechanical Testing on Resistance Spot Weld Nuggets of AISI 316L Stainless Steel Sheets" *International Journal of Aerospace, Mechanical, Structural and Mechatronics Engineering* Vol. 1, (2015) ISSN: 2454-4094
17. Vicente Afonso Ventrella, José Roberto Berrettab, Wagner de Rossi "Pulsed Nd:YAG laser seam welding of AISI 316L stainless steel thin foils" *Journal of Materials Processing Technology* 210 (2010) 1838-1843
18. Yazdipour , A. Heidarzadeh "Effect of friction stir welding on microstructure and mechanical properties of dissimilar Al 5083-H321 and 316L stainless steel alloy joints", *Journal of Alloys and Compounds* 680 (2016) 595e603
19. Manish P. Meshram, Basanth Kumar Kodli, Subhash R. Dey "Mechanical properties and Microstructural Characterization of friction stir welded AISI 316 Austenitic Stainless Steel", *International Conference on Advances in Manufacturing and Materials Engineering, AMME* 2014.
20. Y. Lekhana, A. Nikhila, K. Bharath, B. Naveen, A. Chennakesava Reddy "Weldability Analysis of 316 Stainless Steel and AA1100 Alloy Hollow Tubes using Rotational Friction Welding Process", *International Journal of Science and Research (IJSR)* ISSN (Online): 2319-7064, Volume 5 Issue 5, May 2016
21. Sirajuddin Elyas Khany, S.N. Mehdi, G.M. Sayeed Ahmed "An Analytical Study of Dissimilar Materials Joint Using Friction Welding and It's Application" - *International Journal of Scientific and Research Publications*, Volume 5, Issue 2, February 2015, ISSN 2250-3153
22. Gourav Sardana, Ajay Kumar "To Study the Mechanical Behaviour of Friction Welding of HSS M33 & SS 316", [IJESAT] [*International Journal of Engineering Science & Advanced Technology*] Volume-3, Issue-4, 131-134
23. Manish P. Meshram, Basanth Kumar Kodli, Suhash R. Dey "Friction Stir Welding of Austenitic Stainless Steel by PCBN Tool and Its Joint Analyses" , 3rd International Conference on Materials Processing and Characterisation (ICMPCE 2014)
24. Basil Thorns, Cijo Mafew "Study on the Effect of Tool Material on Mechanical Properties and Microstructures of Friction Stir Welded AA 6061 Aluminum Alloy" , *International Journal of Latest Trends in Engineering and Technology (IJLTET)*
25. M. Jandaghi, P. Parvin, M. J. Torkamany, J. Sabbaghzadeh " Alloying elemental change of SS-316 and Al-5754 during laser welding using real time laser induced breakdown spectroscopy (LIBS) accompanied by EDX and PIXE microanalysis", *LANE* 2010.
26. Qixian Zheng, Xiaomei Feng, Yifu Shen, Guoqiang Huang, Pengcheng Zhao " Dissimilar friction stir welding of 6061 Al to 316 stainless steel using Zn as a filler metal", *Journal of Alloys and Compounds* 686 (2016) 693e701
27. K.C. Ganesh, M. Vasudevan, K.R. Balasubramanian, N. Chandrasekhar, S. Mahadevan, P. Vasantharaja and T. Jayakumar, "Modeling, Prediction and Validation of Thermal Cycles, Residual Stresses and Distortion in type 316 LN Stainless Steel Weld Joint made by TIG Welding Process", 1st International Conference on Structural Integrity, ICONS-2014, *Procedia Engineering* 86 ( 2014 ) 767 - 774
28. Devaraju- "An Experimental study on TIG welded joint between Duplex Stainless Steel and 316L Austenitic Stainless Steel (2015)" *SSRG International Journal of Mechanical Engineering (SSRG-IJME)*, ISSN: 2348 - 8360
29. Ajay S. Karwande, Rameshwar V. Chavan, J. J. Salunke, - "Experimental Investigation of SS 316LN by using TIG-MAG Welding", *IJSEC* (2016), ISSN 2321 3361
30. K. C. Ganesh , M. Vasudevan , K. R. Balasubramanian , N. Chandrasekhar & P. Vasantharaja "Thermo-mechanical Analysis of TIG Welding of AISI 316LN Stainless Steel", *Materials and Manufacturing Processes*, 29: 903-909, Taylor & Francis Group, LLC ISSN: 1042-6914
31. Harish Kumar D, A. Somireddy, K. Gururaj "A review on critical aspects of 316LN austenitic stainless Steel weldability", *International Journal of Materials Science and Applications*, 2012; 1(1):1-7
32. E. Ahmadi, A.R. Ebrahimi "The Effect of Activating Fluxes on 316L Stainless Steel Weld Joint Characteristic in TIG Welding Using the Taguchi Method", *Journal of Advanced Materials and Processing*, Vol. 1, No. 1, 2013, 55-62.

33. M. Dadfar , M.H. Fathi, F. Karimzadeh, M.R. Dadfar, A. Saatchi - "Effect of TIG welding on corrosion behaviour of 316L stainless steel", Materials Letters (2007), ISSN: 2343–2346

34. E. Ahmadi and A.R. Ebrahimi "Welding of 316L Austenitic Stainless Steel with Activated Tungsten Inert Gas

Process(2015)" Journal of Materials Engineering and Performance ,ISSN: 1065–1071.

35. P Sakhivel, P Sivakumar "Effect of Vibration in TIG and Arc Welding Using AISI 316 Stainless Steel (2014)", International Journal Of Engineering Research and Science and Technology, ISSN 2319-5991.